SOME MEMORIES ABOUT THE SEARCH OF NON-ABELIAN GAUGE FIELDS IN GRAPHENE MATERIALS

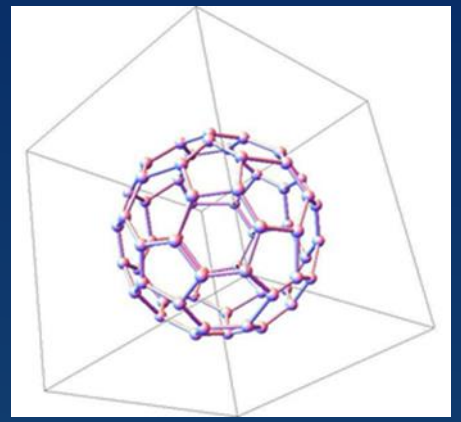

J. González
Instituto de Estructura de la Materia, CSIC, Spain

Some memories about the prehistory

VOLUME 69, NUMBER 1 PHYSICAL REVIEW LETTERS 6 JULY 1992

Continuum Approximation to Fullerene Molecules

José González,[1] Francisco Guinea,[2],[a] and M. Angeles H. Vozmediano[1]

[1]*Instituto de Física Fundamental, Consejo Superior de Investigaciones Científicas, Serrano 123, 28006 Madrid, Spain*
[2]*The Harrison M. Randall Laboratory of Physics, The University of Michigan, Ann Arbor, Michigan 48109-1120*
(Received 17 March 1992)

The electronic and elastic properties of large fullerene molecules are studied. The low-lying electronic levels are described by the Dirac equations in (2+1) dimensions, and the intramolecular modes are given by the theory of elasticity. Coupling between electrons and phonons can also be written in a simple way. The quantum dynamics of the ions is modified by the appearance of nontrivial Berry's phases. The qualitative features of fullerenes with elliptical and cylindrical geometries, and minimal surfaces with negative curvature are also studied.

Fullerene molecules are spherical cages made of carbon atoms, which may come with an increasing size

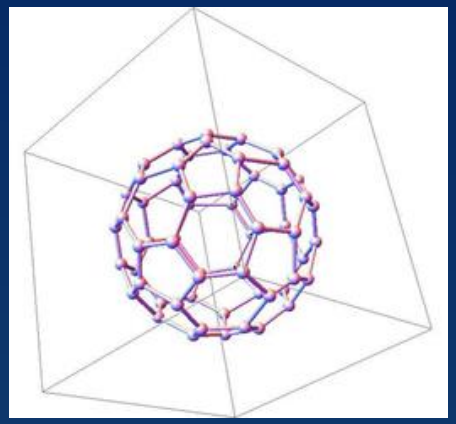
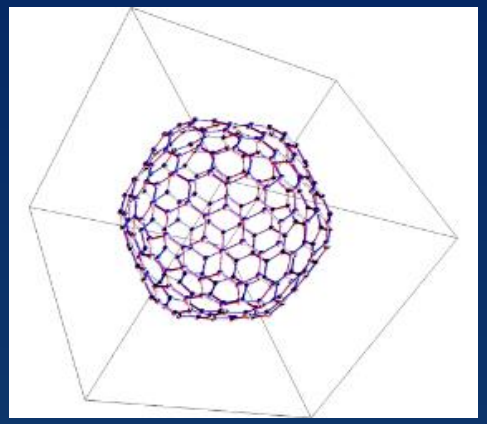
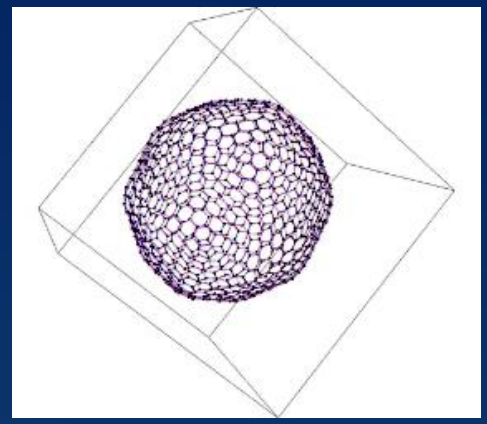

They all come with 12 pentagonal rings, which is enforced by the Euler theorem

$$\chi = \#\text{vertices} - \#\text{edges} + \#\text{faces} = 2$$

Indeed, the contribution of an hexagon to the Euler characteristic is

$$\Delta\chi = \frac{6}{3} - \frac{6}{2} + 1 = 0$$

while the contribution of a pentagon is

$$\Delta\chi = \frac{5}{3} - \frac{5}{2} + 1 = \frac{1}{6}$$

But the amazing feature of fullerenes is their low-energy electronic spectrum

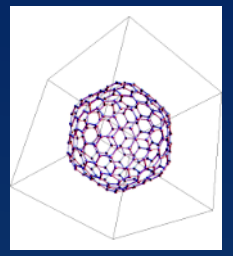

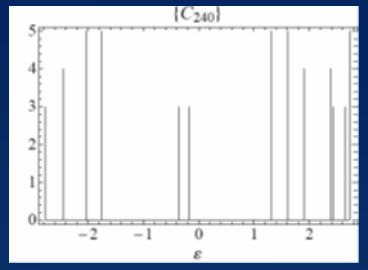

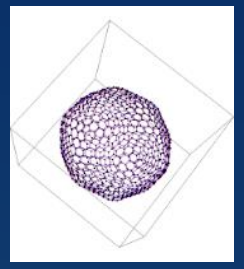

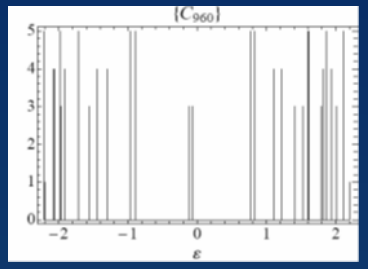

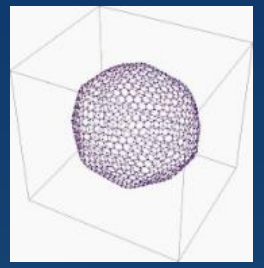

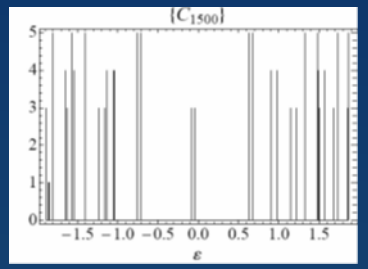

The electronic spectra of the series of very large fullerenes are remarkable, as one recovers the degeneracy of the multiplets of the angular momentum (3, 5, 7, …), but $l = 1$ turns out to be the lowest possible value.

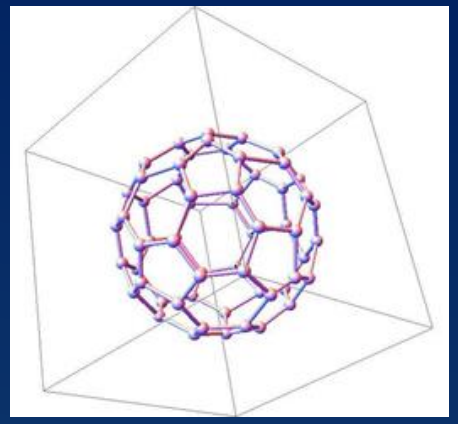
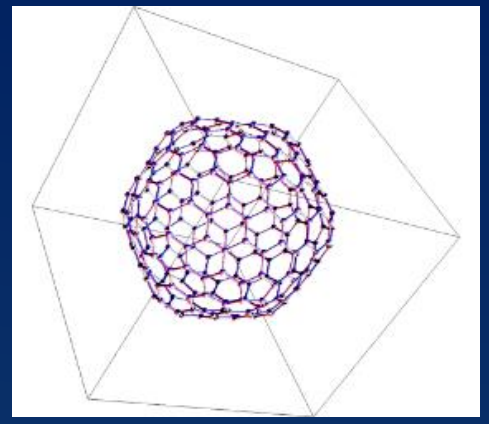
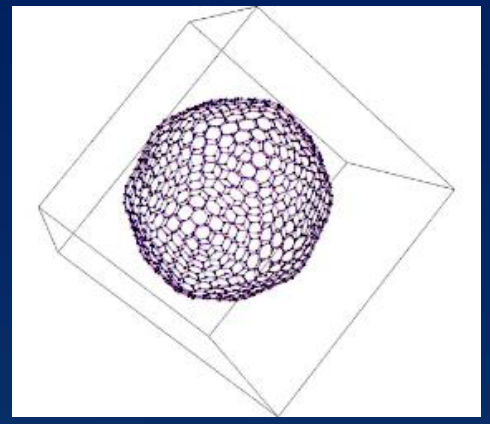

If the rotational symmetry is realized approximately for very large fullerenes, it seems that the Dirac equation on the surface of a sphere should give a sensible description of the spectrum

$$i\,\sigma\cdot\nabla\,\Psi_n \;=\; \varepsilon_n\,\Psi_n$$

However, the Dirac equation on the surface of a sphere does not have zero modes, while the spectrum is given in terms of the total angular momentum j

$$\varepsilon_j = \pm\left(j+\frac{1}{2}\right)\frac{1}{R}$$

The resolution of the puzzle comes from the observation that the pentagonal defects do more that just adding curvature to the surface.

The pentagonal carbon rings can be formed by making a cut in the plane and gluing the edges. This induces an effective rotation of $\pi/3$ at the junction, which implies in turn the exchange of the two Dirac valleys

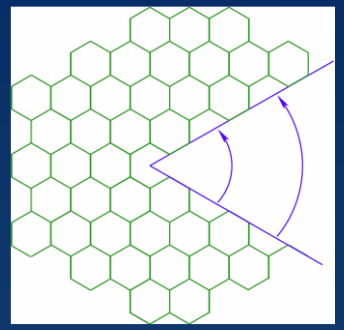

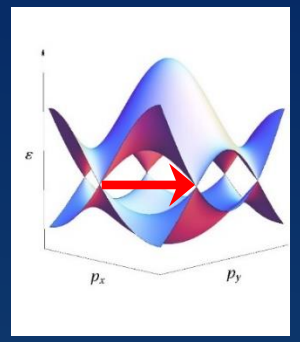

The exchange of the two Dirac valleys is only felt when making a complete turn around the topological defect. Therefore, the effect can be mimicked by a line of effective gauge flux Φ threading the pentagonal ring, acting on the $(K\,,K')$ space

$$A_\theta = \frac{\Phi}{2\pi}\begin{pmatrix} 0 & -i \\ i & 0 \end{pmatrix}$$

$$\exp\left(i\oint d\theta\, A_\theta\right)\begin{pmatrix}\psi_K \\ \psi_{K'}\end{pmatrix} = \begin{pmatrix} 0 & 1 \\ -1 & 0 \end{pmatrix}\begin{pmatrix}\psi_K \\ \psi_{K'}\end{pmatrix} \qquad \Rightarrow \qquad \Phi = \frac{\pi}{2}$$

J. G., F. Guinea and M.A.H. Vozmediano, Nucl. Phys. B 406, 771 (1993)

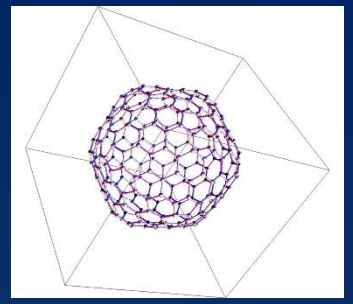

In the fullerenes, the combined effect of the 12 pentagonal rings is consistent with the field of a monopole, whose charge is dictated by the total flux

$$g = \frac{1}{4\pi} \sum_{i=1}^{12} \frac{\pi}{2} = \frac{3}{2}$$

By approximating the effective gauge field by an isotropic flux at the spherical surface of the fullerene, the Dirac equation for the curved lattice becomes

$$i\boldsymbol{\gamma} \cdot (\nabla - i\mathbf{A})\, \Psi_n = \varepsilon_n\, \Psi_n$$

where $\mathbf{A}$ is the effective gauge field mixing the spinors at K and K'.

The problem can be solved by passing to the operator $\mathbf{J}$ of the total angular momentum of spinors, curvature and gauge field, which leads to the equation

$$\left(\mathbf{J}^2 + \frac{1}{4} - g^2 \right) \Psi_n = \varepsilon_{\mathrm{n}}^2\, R^2\, \Psi_n$$

The spectrum is then given in terms of the angular momentum number j

$$\varepsilon_j^2\, R^2 = \left(j + \frac{1}{2} \right)^2 - g^2$$

which, for $g = 3/2$, accounts for the existence of two triplets of zero modes with $j = 1$.

Other instances where topological defects arise in graphene correspond to geometries with negative curvature. We have in particular the case of nanotube-graphene junctions

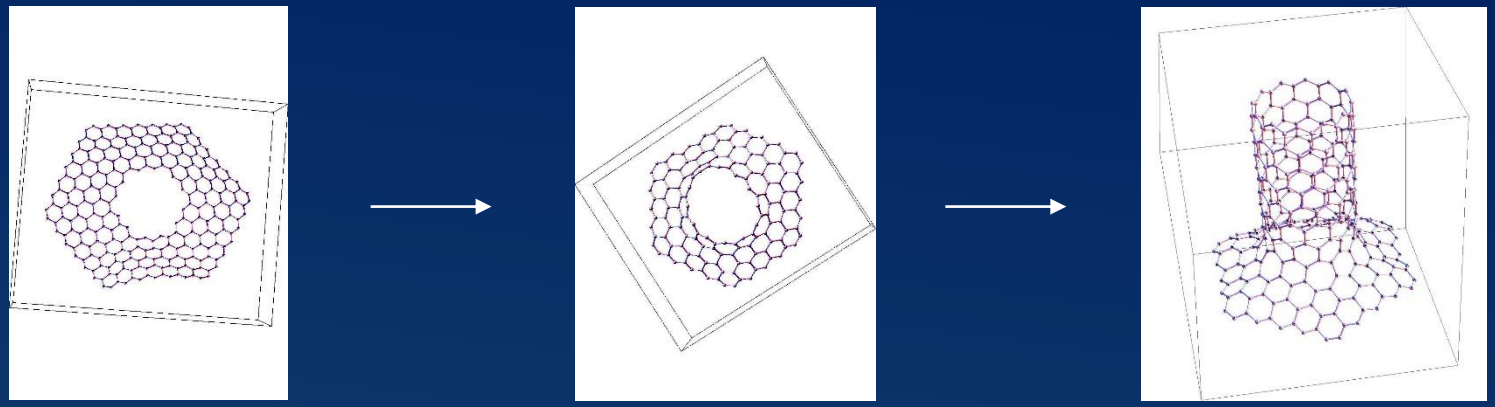

This corresponds to a surface with Euler characteristic $\chi = \frac{1}{4\pi}\int d^2x\sqrt{g}\,R = -1$

So we must have $\chi = \#\text{vertices} - \#\text{edges} + \#\text{faces} = -1$

The contribution of each heptagon is now given by

$$\Delta\chi = \frac{7}{3} - \frac{7}{2} + 1 = -\frac{1}{6}$$

Which means that we must have 6 heptagons to reach the Euler characteristic $\chi = -1$.

When the heptagonal rings are regularly distributed at the junction, the possible geometries correspond to nanotubes of type $(6n,6n)$ ("armchair"), or type $(6n,0)$ ("zigzag").

$(6n,6n)$

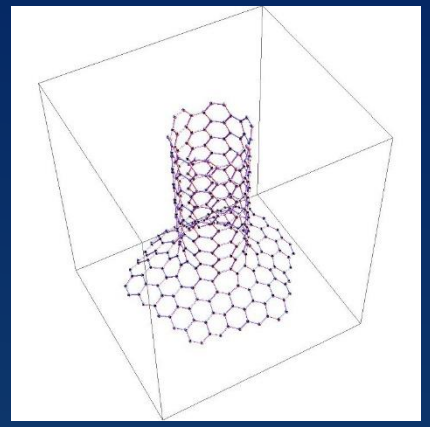

$(6n,0)$

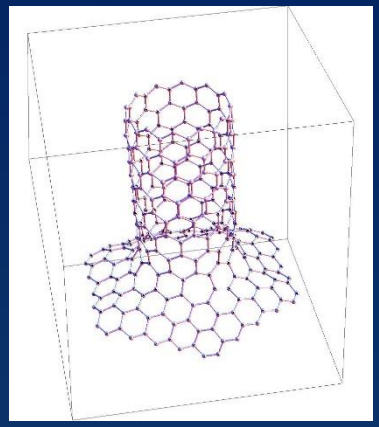

When looking at the electronic spectra, it can be seen that all the $(6n,6n)$ geometries have a peak at zero energy in the local density of states at the junction, while this also happens in the $(6n,0)$ geometries when n is a multiple of 3

(18,0)

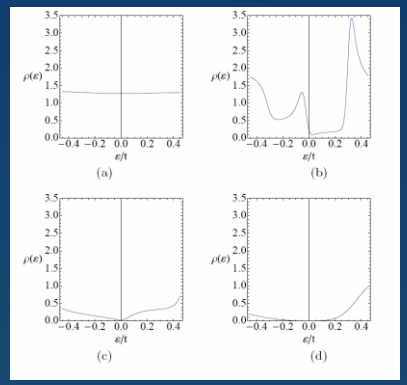

(54,0)

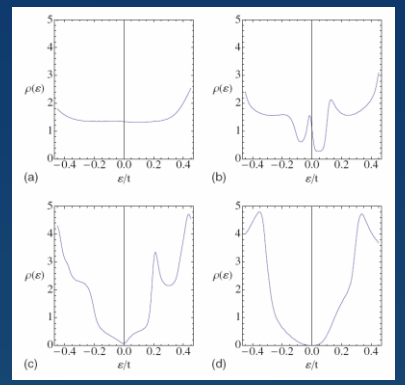

J. G., F. Guinea and J. Herrero, Phys. Rev. B 79, 165434 (2009)

(local DOS shown here for different quantum number under $\pi/3$ rotation, $q = 1\ (a),\ e^{\pm\frac{i\pi}{3}}\ (b),\ e^{\pm\frac{2i\pi}{3}}\ (c),\ -1\ (d)$)

The low-energy electronic spectrum can be approached by solving the Dirac equation in the nanotube and graphene sides, and then matching the solutions at the junction

$$iv_F\boldsymbol{\sigma}\cdot\left(\nabla \mp ie\mathbf{A}\right)\Psi^{\pm} = \varepsilon\,\Psi^{\pm}$$

$$\begin{aligned} iv_F\left(\partial_r + \frac{i\partial_\theta}{r} \pm \frac{\Phi}{r} + \frac{1}{2r}\right)\Psi_A^{\pm}(r,\theta) &= \varepsilon\Psi_B^{\pm}(r,\theta) \\ iv_F\left(\partial_r - \frac{i\partial_\theta}{r} \mp \frac{\Phi}{r} + \frac{1}{2r}\right)\Psi_B^{\pm}(r,\theta) &= \varepsilon\Psi_A^{\pm}(r,\theta) \end{aligned}$$

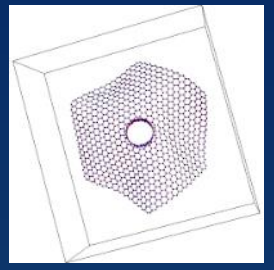

$$\begin{aligned} iv_F\left(\partial_z + \frac{i\partial_\theta}{R_0}\right)\Psi_A^{\pm}(z,\theta) &= \varepsilon\Psi_B^{\pm}(z,\theta) \\ iv_F\left(\partial_z - \frac{i\partial_\theta}{R_0}\right)\Psi_B^{\pm}(z,\theta) &= \varepsilon\Psi_A^{\pm}(z,\theta) \end{aligned}$$

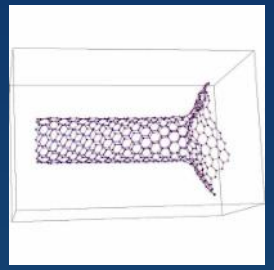

This model has indeed solutions at $\varepsilon = 0$ when the fictitious gauge flux is above certain minimum value

$$i\begin{pmatrix} 0 & \partial_r - \frac{1}{r} i\partial_\theta \mp \frac{\Phi}{2\pi r} + \frac{1}{2r} \\ \partial_r + \frac{1}{r} i\partial_\theta \pm \frac{\Phi}{2\pi r} + \frac{1}{2r} & 0 \end{pmatrix} \begin{pmatrix} \Psi_A^{\pm} \\ \Psi_B^{\pm} \end{pmatrix} = 0$$

Adding the gauge flux of the 6 heptagonal rings up to $\Phi = 3\pi$, we get zero modes of the form

$$\Psi_A^+ \sim r^{n-\Phi/2\pi-1/2}\, e^{in\theta} \quad , \ \Psi_B^+ = 0 \qquad r > R_0$$
$$\Psi_A^+ \sim e^{n(z/R_0)}\, e^{in\theta} \quad , \ \Psi_B^+ = 0 \qquad z < 0$$

We find a state with $n = 1$ which has an amplitude decaying in both the plane and the nanotube. Similarly, we have another localized state with $n = -1$ in the other sublattice of the graphene layer. These localized states are then consistent with the above low-energy peak in the DOS.

(12,12)

$q = e^{\pm i\pi/3}$

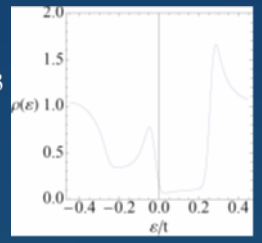

(18,0)

$q = e^{\pm i\pi/3}$

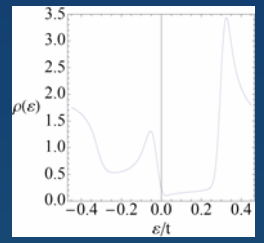

One can also deal with a regular lattice of nanotube-graphene junctions, as an ideal form of some structures which have been synthesized in the lab

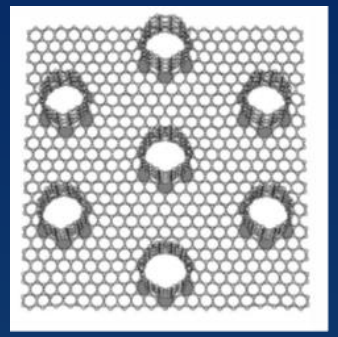

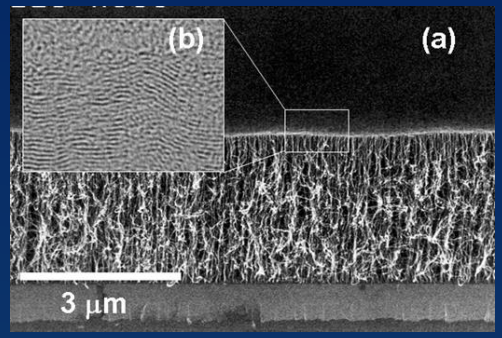

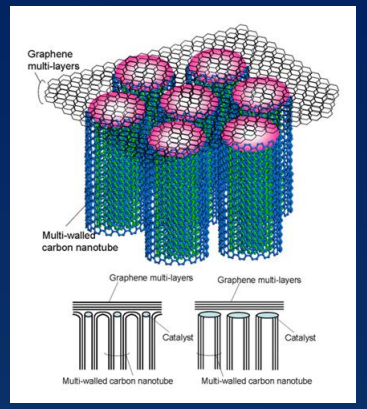

(from Fujitsu Laboratories Ltd.)

Taking in particular a lattice of junctions with armchair nanotubes, or (6*n*,0) tubes *n* being a multiple of 3, we find flat bands close to the Fermi level, which are a reflection of the localized modes at the junctions

(12,12)

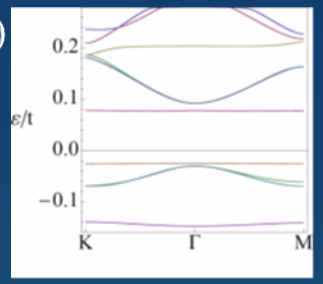

(18,0)

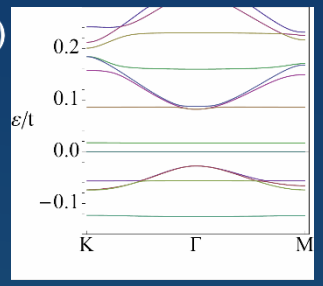

J. G., F. Guinea and J. Herrero, Phys. Rev. B 79, 165434 (2009)

Memories about more recent history

PRL **108,** 216802 (2012) PHYSICAL REVIEW LETTERS week ending 25 MAY 2012

Non-Abelian Gauge Potentials in Graphene Bilayers

P. San-Jose,[1] J. González,[1] and F. Guinea[2]

[1]*Instituto de Estructura de la Materia (IEM-CSIC), Serrano 123, 28006 Madrid, Spain*
[2]*Instituto de Ciencia de Materiales de Madrid (ICMM-CSIC), Cantoblanco, 28049 Madrid, Spain*

(Received 17 October 2011; published 23 May 2012)

We study the effect of spatial modulations in the interlayer hopping of graphene bilayers, such as those that arise upon shearing or twisting. We show that their single-particle physics, characterized by charge accumulation and recurrent formation of zero-energy bands as the pattern period L increases, is governed by a non-Abelian gauge potential arising in the low-energy electronic theory due to the coupling between layers. We show that such gauge-type couplings give rise to a potential that, for certain discrete values of L, spatially confines states at zero energy in particular regions of the moiré patterns. We also draw the connection between the recurrence of the flat zero-energy bands and the non-Abelian character of the potential.

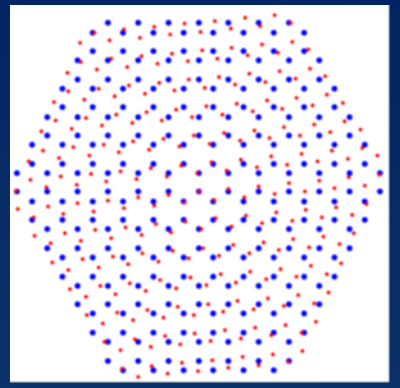

It is possible to form commensurate superlattices from a graphene bilayer by means of a relative twist

We have a sequence of superlattices with

$$\cos(\theta_n) = \frac{3n^2 + 3n + 1/2}{3n^2 + 3n + 1}$$

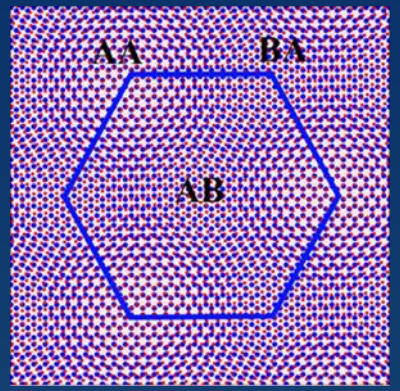

This gives rise to a superlattice with a periodic pattern of regions with *AA*, *AB* and *BA* stacking. Along the mentioned sequence, we have a growing period

$$L_n = \sqrt{3n^2 + 3n + 1}$$

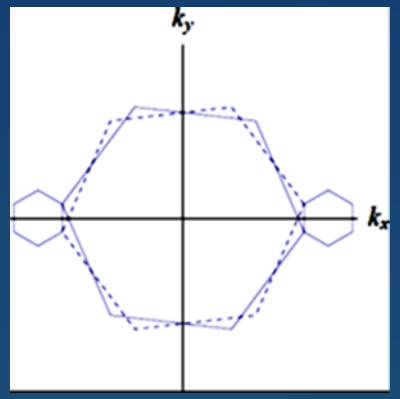

In momentum space, we have two inequivalent moiré Brillouin zones which arise from the hybridization of states around the respective *K* valleys, and respective –*K* valleys of the two layers

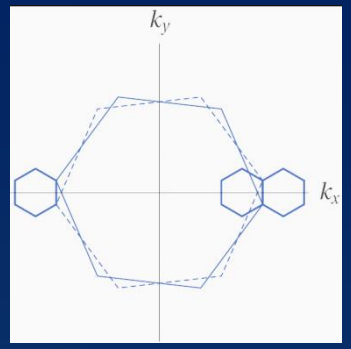

This picture leads in momentum space to the so-called continuum model, accounting for the hybridization of states at valley $\boldsymbol{K}$, layer 1, with states at valley $\boldsymbol{K}$ - $\boldsymbol{\Delta K}$, $\boldsymbol{K}$ - $\boldsymbol{\Delta K}$ + $\boldsymbol{G}_1$, and $\boldsymbol{K}$ - $\boldsymbol{\Delta K}$ + $\boldsymbol{G}_2$, of layer 2 (J. M. B. Lopes dos Santos, N. M. R. Peres and A. H. Castro Neto, PRL 99, 256802 (2007))

This leads to a smooth modulation of the interlayer hopping $V_{\alpha\beta}(\mathbf{r}) = \frac{w}{v_F}\sum_{j=1}^{3} e^{i\mathbf{Q}_j\cdot\mathbf{r}}$ $\mathbf{Q}_1 = \mathbf{0}$, $\mathbf{Q}_2 = \mathbf{G}_1$, $\mathbf{Q}_3 = \mathbf{G}_2$

$$H = v_F \begin{pmatrix} 0 & -i(\partial_x - i\partial_y) - i\frac{\Delta K}{2} & V_{AA'}(\mathbf{r}) & V_{AB'}(\mathbf{r}) \\ -i(\partial_x + i\partial_y) + i\frac{\Delta K}{2} & 0 & V_{BA'}(\mathbf{r}) & V_{BB'}(\mathbf{r}) \\ V^*_{AA'}(\mathbf{r}) & V^*_{BA'}(\mathbf{r}) & 0 & -i(\partial_x - i\partial_y) + i\frac{\Delta K}{2} \\ V^*_{AB'}(\mathbf{r}) & V^*_{BB'}(\mathbf{r}) & -i(\partial_x + i\partial_y) - i\frac{\Delta K}{2} & 0 \end{pmatrix}$$

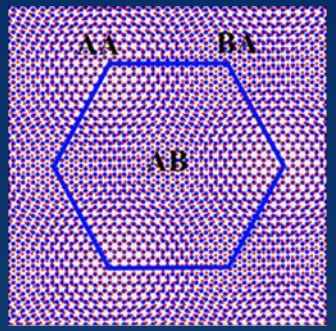

This continuum model allows to understand many of the low-energy properties of twisted bilayer graphene

$n = 10$ 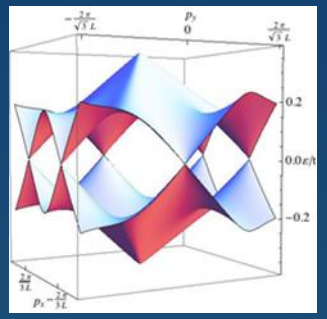

$n = 22$ 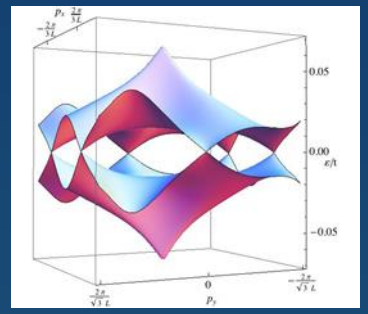

$n = 25$ 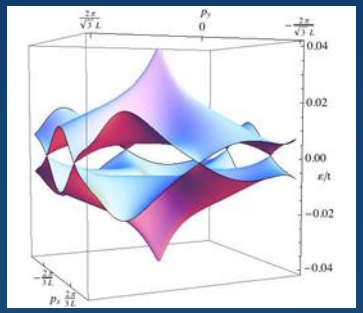

One of the first effects derived from the continuum model was the strong renormalization of the Fermi velocity v_F (J. M. B. Lopes dos Santos, N. M. R. Peres and A. H. Castro Neto, PRL 99, 256802 (2007))

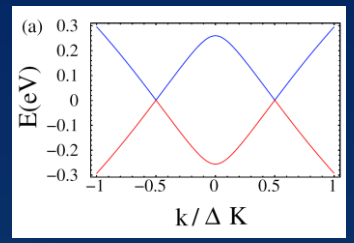

$$\frac{v^*}{v_F} \approx 1 - 9\left(\frac{w}{v_F \Delta K}\right)^2 + \ldots$$

The measure of the separation between the van Hove singularities in valence and conduction bands made possible and accurate determination of the renormalization

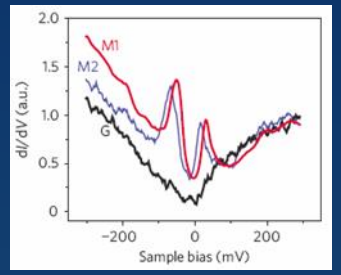

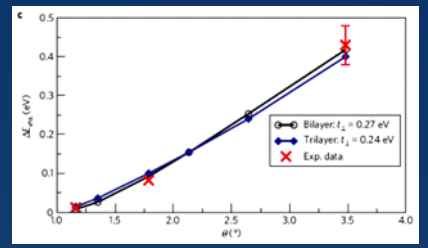

G. Li *et al.*, Nature Phys. 6, 109 (2010)

Other experiments carried out with STS were indeed observing the breakdown of single layer behavior

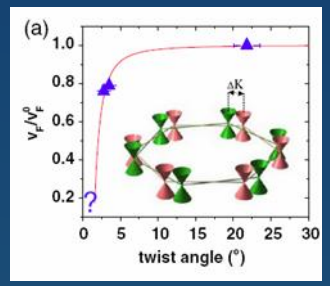

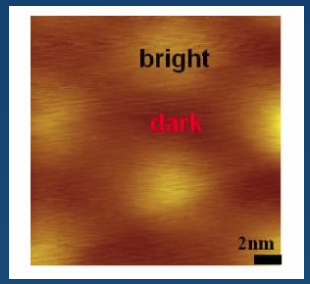

A. Luican *et al.*, Phys. Rev. Lett. 106, 126802 (2011)

Relying on the continuum model, it was shown that the Fermi velocity should be renormalized according to the exact formula (R. Bistritzer and A. H. MacDonald, PNAS 108, 12233 (2011))

$$\frac{v^*}{v_F} = \frac{1-3\alpha^2}{1+6\alpha^2} \quad , \qquad \alpha = \frac{w}{v_F \Delta K}$$

The point at which v_F vanishes ("magic" angle) signals the development of an approximately flat band

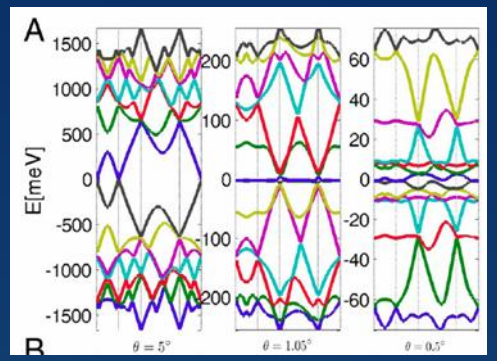

It was actually found that there is a whole sequence of magic angles at which v_F vanishes

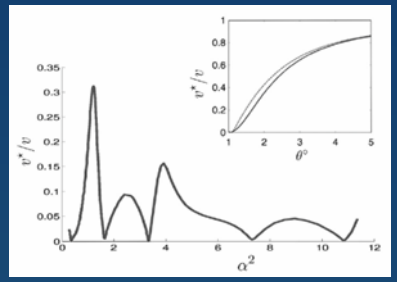

(R. Bistritzer and A. H. MacDonald, PNAS 108, 12233 (2011))

In an attempt to understand the physics of the magic angles, we pursued the approach of casting the continuum model in terms of gauge fields (P. San-José, J. G. and F. Guinea, PRL **108**, 216802 (2012))

This can be more easily illustrated in a model with real interlayer potentials, with

$$V_{AB'} = -A_x - A_y \quad , \quad V_{BA'} = -A_x + A_y$$

$$H = v_F \begin{pmatrix} 0 & -i(\partial_x - i\partial_y) & V_{AA'}(\mathbf{r}) & V_{AB'}(\mathbf{r}) \\ -i(\partial_x + i\partial_y) & 0 & V_{BA'}(\mathbf{r}) & V_{BB'}(\mathbf{r}) \\ V_{AA'}(\mathbf{r}) & V_{BA'}(\mathbf{r}) & 0 & -i(\partial_x - i\partial_y) \\ V_{AB'}(\mathbf{r}) & V_{BB'}(\mathbf{r}) & -i(\partial_x + i\partial_y) & 0 \end{pmatrix} = v_F \begin{pmatrix} 0 & -i(\partial_x - i\partial_y) & \phi & -A_x - A_y \\ -i(\partial_x + i\partial_y) & 0 & -A_x + A_y & \phi \\ \phi & -A_x + A_y & 0 & -i(\partial_x - i\partial_y) \\ -A_x - A_y & \phi & -i(\partial_x + i\partial_y) & 0 \end{pmatrix}$$

A_x and A_y induce a shift of the momenta, which is off-diagonal in the space of the two layers

$$H = v_F \begin{pmatrix} \sigma_x & \sigma_y \end{pmatrix} \cdot \begin{pmatrix} -i\partial_x - A_x\tau_1 \\ -i\partial_y - A_y\tau_2 \end{pmatrix} + v_F \phi \tau_1$$

The case of twisted bilayer graphene is more involved since the interlayer potentials are complex and we have the mismatch ΔK in the position of the Dirac nodes

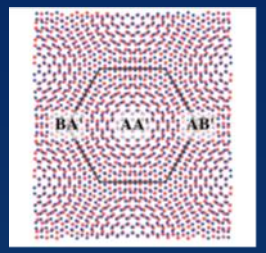

$$H = v_F \begin{pmatrix} 0 & -i(\partial_x - i\partial_y) - i\Delta K/2 & V_{AA'}(\mathbf{r}) & V_{AB'}(\mathbf{r}) \\ -i(\partial_x + i\partial_y) + i\Delta K/2 & 0 & V_{BA'}(\mathbf{r}) & V_{BB'}(\mathbf{r}) \\ V^*_{AA'}(\mathbf{r}) & V^*_{BA'}(\mathbf{r}) & 0 & -i(\partial_x - i\partial_y) + i\Delta K/2 \\ V^*_{AB'}(\mathbf{r}) & V^*_{BB'}(\mathbf{r}) & -i(\partial_x + i\partial_y) - i\Delta K/2 & 0 \end{pmatrix}$$

But we can achieve a similar construction

$$V_{AB'} = -A_{1x} + A_{2y} + i(A_{2x} + A_{1y})$$
$$V_{BA'} = -A_{1x} - A_{2y} + i(A_{2x} - A_{1y})$$

Introducing the Pauli matrices τ_i acting on the layer space, we can write in compact form

$$H = v_F \boldsymbol{\sigma} \cdot (-i\partial + \tau_3 \Delta\mathbf{K}/2 - \hat{\mathbf{A}}) + v_F \hat{\Phi} \qquad \hat{\mathbf{A}} = \begin{pmatrix} A_{1x}\tau_1 + A_{2x}\tau_2 \\ A_{1y}\tau_1 + A_{2y}\tau_2 \end{pmatrix}$$

$$\hat{\Phi} = \mathrm{Re}(V_{AA'})\,\tau_1 - \mathrm{Im}(V_{AA'})\,\tau_2$$

We can remove the $\Delta\mathbf{K}$ mismatch of the Dirac cones by means of a gauge transformation

$$\Psi = e^{-i\tau_3 \frac{\Delta\mathbf{K}}{2}\cdot\mathbf{r}} \tilde{\Psi} \qquad \Rightarrow \qquad H = v_F \boldsymbol{\sigma} \cdot (-i\partial - \hat{\mathbf{A}}) + v_F \hat{\Phi}$$

P. San-José, J. G. and F. Guinea, PRL **108**, 216802 (2012)

By squaring the Dirac equation, we obtain (at $\Phi = 0$)

$$v_F^2\left(-\partial^2 + i\partial\cdot\hat{\mathbf{A}} + 2i\hat{\mathbf{A}}\cdot\partial + \hat{\mathbf{A}}^2 - \sigma_z\hat{F}_{xy}\right)\Psi = \varepsilon^2\,\Psi$$

The pattern of confinement can be read from the vector potential, which keeps the charge density away from the regions of stacking *AB′* or *BA′*

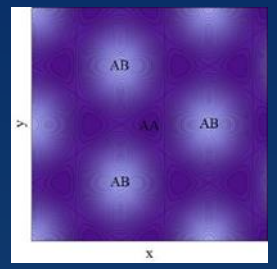

$$(A_{1x} \pm A_{2y})^2 + (A_{2x} \mp A_{1y})^2$$

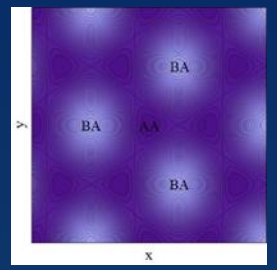

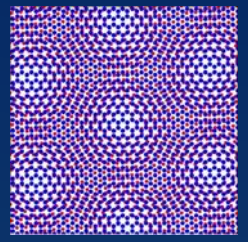

However, it is much more difficult to establish a quantization rule that may explain the sequence of magic angles --perhaps commensuration of the flux in the moiré unit cell?

Anyhow, it turned out that, at large *L*, the sequence is given by the formula

$$\frac{wL_n}{v_F} = 2\pi\, c\left(n + \frac{1}{2}\right)$$

P. San-José, J. G. and F. Guinea, PRL **108**, 216802 (2012)